Indonesian Journal of Material Research
e-ISSN: 2987-1654
Vol. 4, No. 2, July 2026

Indonesian Journal of MATERIAL RESEARCH

Research Paper

Effect from Fluorization Upon Formation as Well as Luminescence for ZrO_2:Eu Nanogranules

Nguyen Thi Phuong Loan[1*]

[1] *Faculty of Fundamental 2, Posts and Telecommunications Institute of Technology, Ho Chi Minh City, 70000, Vietnam*
[*] **Corresponding author**: ntploan@ptithcm.edu.vn

Abstract
ZrO_2:Eu phosphor materials were synthesized using a solid-state reaction method in order to investigate their structural and luminescent properties. The obtained powder samples were systematically characterized by X-ray diffraction (XRD), scanning electron microscopy (SEM), and photoluminescence (PL) spectroscopy. XRD patterns of all Eu-doped samples reveal the coexistence of monoclinic and cubic phases of ZrO_2, indicating that phase transformation occurs during the high-temperature solid-state synthesis process. The results further suggest that the samples undergo crystallization in a dense solid form. SEM observations confirm the formation of aggregated crystalline particles with relatively uniform morphology. At room temperature, the PL spectra of all investigated samples exhibit a broad emission band attributed to host-related luminescence, along with distinct sharp emission peaks corresponding to the characteristic radiative transitions of Eu^{3+} ions under optical excitation. Notably, the overall luminescence intensity of Eu^{3+} increases by at least six times with increasing fluorine content, demonstrating the strong influence of fluorine incorporation on the optical performance of the phosphor. Possible mechanisms responsible for the enhanced luminescence behavior, including changes in local crystal field symmetry and defect-related energy transfer processes, are discussed. These findings highlight the potential of ZrO_2:Eu materials for photonic and luminescent applications.

Keywords
$Ca_{14}Mg_2(SiO_4)_8$: Eu^{2+}, High Luminous Flux, Color Quality, Green-Emitting Phosphor, White Light Emitting Diodes

Received: 7 January 2026, Accepted: 1 March 2026
https://doi.org/10.26554/ijmr.20264282

1. INTRODUCTION

ZrO_2 exhibits desirable optical, electrical, physical, and thermal attributes among oxide materials, making it a particularly important substance for advanced functional applications. Both undoped and rare-earth-doped ZrO_2 nanogranules have been extensively investigated as luminescent materials due to their chemical stability, wide bandgap, and ability to host optically active ions (Anh et al., 2025). Based on earlier research, ZrO_2 doped with Eu^{3+} or Pr^{3+} can be employed as fluorescent indicators for medical and biological purposes. Notably, rare-earth-doped ZrO_2 as well as Y-stabilized rare-earth ZrO_2 fluorescent nanogranules demonstrate good biocompatibility, chemical stability in physiological environments, and strong luminescent emission. Consequently, enhancing photoluminescence (PL) intensity and tailoring the PL spectra of rare-earth-doped ZrO_2 are of particular interest for both fundamental studies and practical applications (Le et al., 2026; Cong and Anh, 2025; Cong et al., 2025).

A common strategy for modifying the PL properties of nanogr anules is to alter their crystal structure through the incorporation of suitable impurities. The influence of various dopants on ZrO_2 structure has been examined in numerous studies, primarily focusing on the stability of cubic and tetragonal ZrO_2 phases at ambient temperature. Among the monoclinic, tetragonal, and cubic polymorphs of ZrO_2, the monoclinic phase is thermodynamically stable under ambient conditions (Anh, 2024). However, extensive efforts to stabilize ZrO_2 are driven by the greater technological demand for the cubic and tetragonal phases, which offer superior optical and mechanical properties compared with the monoclinic form. Previous studies have shown that incorporating certain oxide additives, such as Y_2O_3, CaO, and related compounds, suppresses the transformation of tetragonal and cubic ZrO_2 into the monoclinic phase, thereby stabilizing the high-temperature tetragonal and cubic polymorphs at room temperature (Le et al., 2025). In addition to alkaline-earth oxides, stabilization of tetragonal and cubic ZrO_2 can also be achieved through the use of rare-earth oxides and rare-earth fluorides. These dopants not only modify phase stability but may also influence defect formation and local crystal fields, which in turn affect the luminescent behavior of rare-earth ions in the ZrO_2 host lattice.

Integrating Eu_2O_3 into ZrO_2 would be particularly appealing

for the stability in the cuboid or tetragonal stages regarding Eu^{3+}. The luminescent nature for the Eu^{3+} discharge focal points within ZrO_2:Eu proves appealing as well. Completely fixated ZrO_2 would be generated with significantly greater quantity for Eu_2O_3. The luminescent irregularities saw extensive research regarding every polymorphic ZrO_2. The concerned stability problems would be linked with supplantation for cation sublatticework which induces oxygen openings caused by charge offsetting (Loan et al., 2025; Ma and Anh, 2024; Trang and Anh, 2025). As such, said openings would be considered one primary element for ZrO_2 stability. Meanwhile, awareness proved to be not as much for the supplantation within the anion sublatticework as well as its effect upon ZrO_2 attributes. Based on assessment from earlier studies, merely certain elements for nitridization as well as fluorization for ZrO_2 nanogranules underwent examination. Regarding ZrO_2 nanogranules integrated with nitrogen, the supplantation O^{2-} via N^{3-} boosts cuboid ZrO_2 stability. On the other hand, nitrogen incorporation boosts alterations within ZrO_2:Eu,N (ZOEN) nanogranules' PL attributes, surpassing those in ZrO_2:Eu nanogranules. Specifically, the luminescence for Eu^{3+} found within non-focal-symmetric location saw augmentation while the whole luminescence intenseness declined under surging N^{3-} presence. Meanwhile, supplementary heat processing for ZOEN boosts the whole PL intenseness twentyfold maximally. Notably, the generation for oxygen openings was projected if nitrogen was integrated. As such, ZrO_2 stability features identical workings regarding the supplantation for cation locations. A different instance for supplantation within the anion formation, the fluorization for ZrO_2, underwent examination merely in terms of significant fluorine quantity as well as synthesizing processes while stage constitution as well as crystalline formations were assessed in Zr−O−F settings. Bare any study is available when it comes to formational as well as PL attributes for ZrO_2 granules integrated with a lesser fluorine quantity as well as joint-integration with Eu^{3+}. The primary goal for the study herein would be uncovering the effect from small fluorine dosage upon formation as well as luminescent attributes, specifically Eu^{3+} luminescent spectrum allocation as well as intenseness, for ZrO_2 granules integrated with Eu. The ZrO_2:Eu/F (ZOEF) granules were created via the solid-state approach with their formation, form as well as PL attributes assessed (Trang et al., 2025; Dung and Anh, 2025; That et al., 2020).

2. EXPERIMENTAL

2.1 Materials and Procedures

The fluorine nanogranule powdered samples for ZrO_2 integrated with Eu were made through the solid-state approach utilizing uncontaminated $ZrO(NO_3)_2 \times {}_2H_2O$, ZrF_4 as well as Eu_2O_3 in the form of preliminary substances (Luo et al., 2020b). Multiple processes were utilized for assessing the effect from Zr/F proportions upon calcinating heat level as well as form yielding multiple hard compounds ZOEF. For making powdered samples as well as eliminating gas joint-substances, the blends for preliminary substances underwent a heating process within four hours then a calcination process under surging heat levels with each level within twenty hours (Thi et al., 2020a,b).

2.2 Instrumentation and Analysis

Considering the intricate luminescent intenseness reliance upon the fluorine dosage, the synthesizing procedure for the sampling units as well as ensuing assessments for attributes as shown in Figure 1 including Xray diffractivity, scanning electronic microscope as well as luminescence were redone thrice. The Xray diffractivity profiles, shown in Figure 1(a), were acquired via one standard powder diffractometric apparatus functioning under Bragg–Brentano form utilizing Ni β-sifted, CuKα radioactivity. The SEM visuals, shown in Figure 1(b), for the powdered samples daubed in gold were acquired via JSM 6060 LV. The PL assessments subject to exciting processes within the UV as well as observable zones were conducted, as exhibited by Figure 1(c). An arc Xenon light as well as spectrometric apparatus were employed in the form of exciting means (Hanh et al., 2021; Luo et al., 2020a). Diffractivity spectrometric apparatus was employed for tracking PL discharge as well as exciting spectra. The PL as well as PL exciting spectra underwent rectification under setting reactions.

Multiple ZrO_2 samples co-doped with Eu were successfully synthesized and systematically analyzed to investigate the influence of fluorine co-doping on their crystalline structure. X-ray diffraction (XRD) patterns obtained from the prepared samples indicate that all fluorine co-doped specimens consist of a mixed-phase structure, comprising both monoclinic and cubic/tetragonal ZrO_2 phases. The differences between the monoclinic and cubic/tetragonal phases were clearly identified by variations in the positions and relative intensities of the characteristic diffraction peaks, including both strong dominant peaks and weaker secondary reflections (Dang et al., 2021). As the fluorine concentration increased, a pronounced change in the XRD profiles was observed. Specifically, the relative intensities of the diffraction peaks associated with the cubic and tetragonal ZrO_2 phases increased progressively, while the peaks corresponding to the monoclinic phase showed a noticeable reduction in intensity. This systematic evolution in peak intensity ratios demonstrates a phase transformation trend induced by fluorine incorporation (Le et al., 2022; Trang, 2022). The results indicate that increasing fluorine content effectively stabilizes the cubic and tetragonal ZrO_2 phases at the expense of the monoclinic phase, leading to a higher proportion of high-symmetry crystal structures within the Eu-doped ZrO_2 samples.

3. RESULTS AND DISCUSSION

The dependence of both intensity and spectral shape of the broad photoluminescence (PL) band in ZOEF was clearly modified with increasing fluorine concentration, indicating that fluorine plays a significant role in governing the emission characteristics. The observed changes in spectral shape further suggest that the origin of this broad PL band involves a complex and multi-component luminescence mechanism rather than a single radiative transition. In fact, the broad PL emission associated with ZrO_2-based systems has been widely recognized as intrinsically complicated.

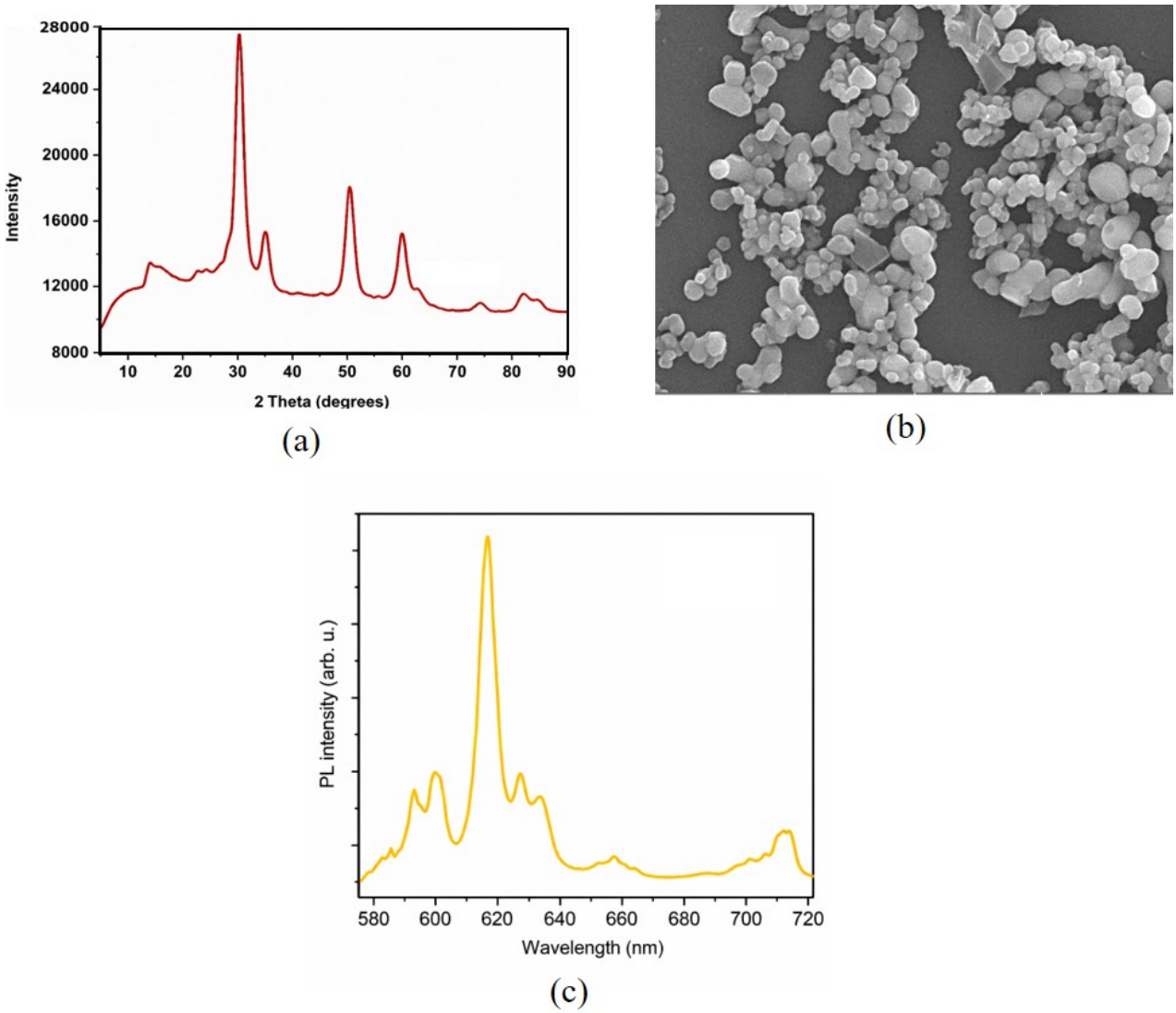

Figure 1. Characterization Data of ZrO_2:Eu: (a) XRD, (b) SEM, and (c) PL Spectroscopy

Previous studies have reported that up to eight individual sub-bands can be deconvoluted within the blue-green spectral region, reflecting the coexistence of multiple defect-related or localized emission centers. The spectral features observed in both the PL emission and excitation processes within the blue–green region allow the identification of a similar luminescence mechanism in hard ZrO_2:Eu^{3+} compounds (ZOE). This suggests that the incorporation of Eu^{3+} ions does not fundamentally alter the nature of the host-related broadband emission, but rather interacts with pre-existing defect or vacancy-related states in the ZrO_2 matrix. However, owing to the highly intricate nature of the ZOE broadband PL emission, the precise origin and contribution of each sub-band remain difficult to unambiguously resolve. The overlap of multiple defect states, charge-compensation mechanisms, and host–dopant interactions leads to a broadened and convoluted spectral profile.

Consequently, while the enhancement and modification of the broadband PL emission with increasing fluorine content can be clearly established, a fully detailed microscopic interpretation remains challenging. At the present stage, only a simplified explanation for the fluorine-induced modification of the ZOE broadband PL can be proposed. This basic interpretation likely involves fluorine-assisted defect formation and charge compensation, which alter the population and radiative efficiency of luminescent centers within the ZrO_2 host lattice. Further spectroscopic and theoretical investigations would be required to disentangle the individual contributions and provide a more comprehensive understanding of the underlying luminescence mechanisms.

The dispersion ratio variations at various wavelengths are shown in Figure 2. When the wavelength grows, the aforementioned factor gradually drops from its highest point, causing

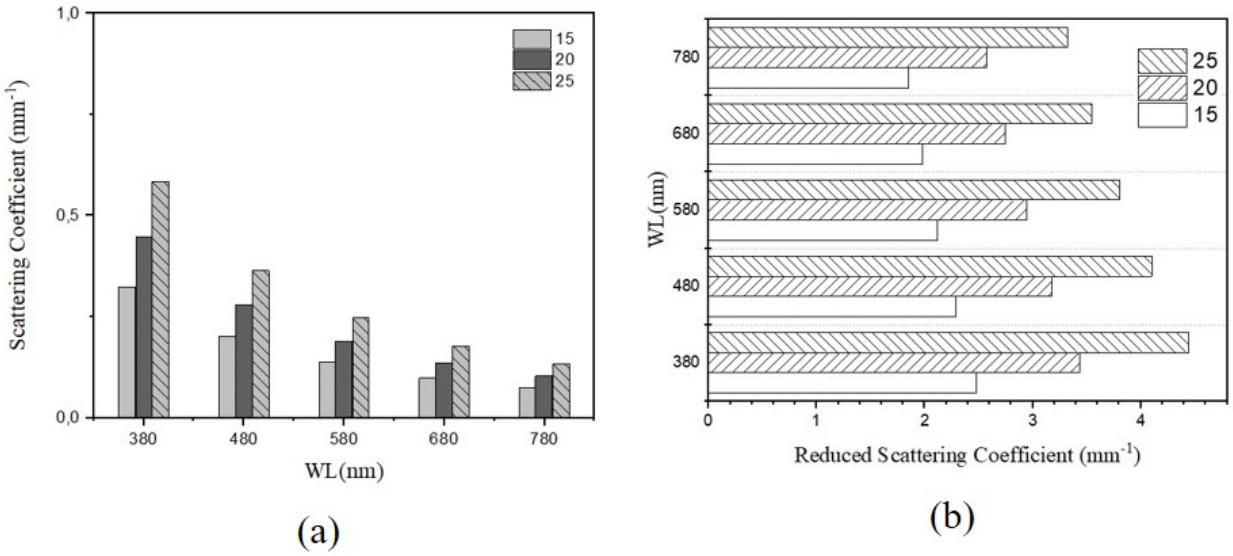

Figure 2. Relationship Between Scattering Coefficient and Wavelength: (a) Scattering Coefficient and (b) Reduced Scattering Coefficient

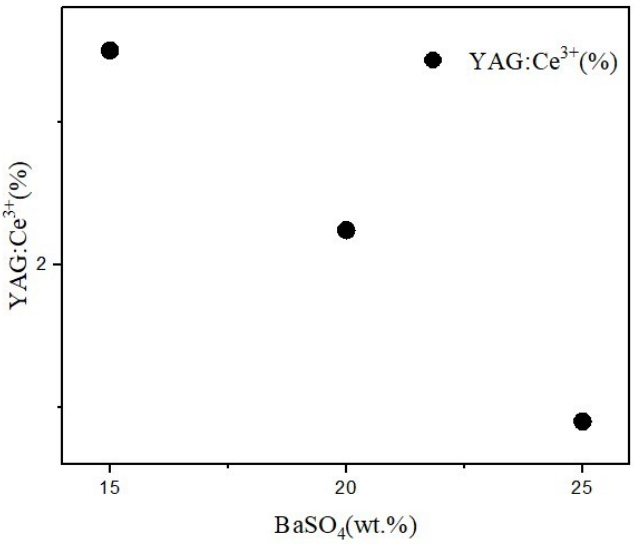

Figure 3. YAG:Ce Presence Interacting with Particle Size of SiO_2

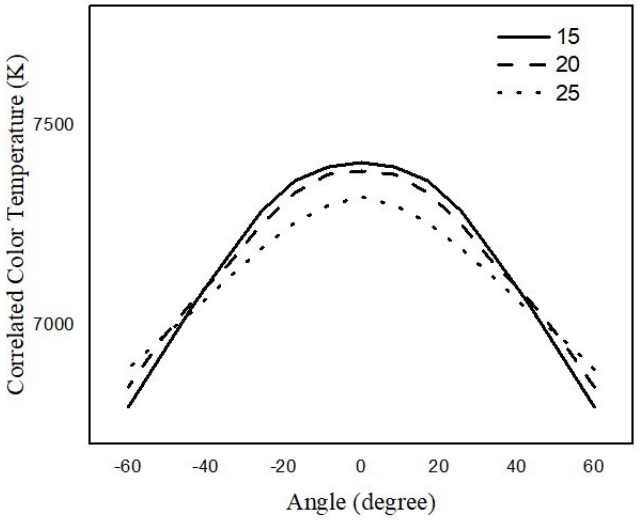

Figure 4. CCT Alteration Based on Particle Size

dispersion for the blue chip's light to move around and eventually transform into rays at longer wavelengths. It seems that an inverse process is responsible for these modifications. The illuminating effect will subsequently rise when the blue-ray dispersion in the front discharge surge decreases along with the blue-ray repeating absorptivity and rear-dispersion. In order to accomplish this, the YAG:Ce ratio must drop as the SiO_2 particle size rises. Figure 3 illustrates how the particle size affects the YAG:Ce amount. As can be observed, the content decreases as SiO_2 particle dimension increases. Figure 4 illustrates how particle size also influences CCT levels. The CCT exhibits discernible variations across all particle sizes. When the particle size is 15 wt.%, the CCT is at its smallest value. On the other hand, the CCT peaks at identical particle size.

Figure 5 illustrates how the color aberration exhibits opposite variations under different particle sizes. Interestingly, the color aberration decreases as the particle size increases but exhibits a notable fall at 20 weight percent. When the particle size increases, the luminosity in the LED depicted in Figure 6 experiences proportionate changes and shows a steady increase. The

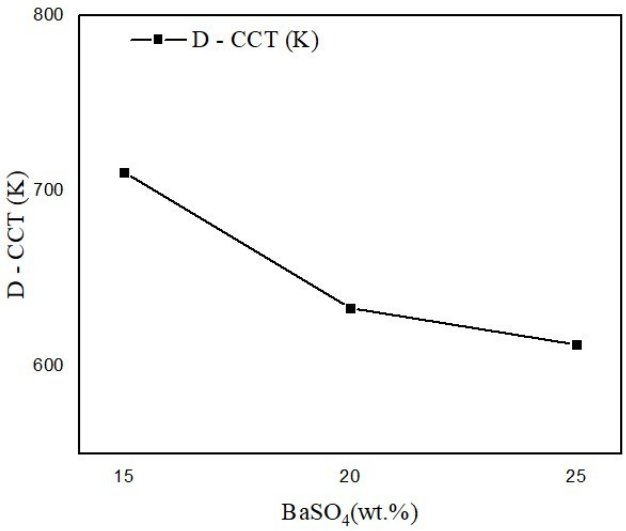

Figure 5. Variation in Hue Aberration Under SiO_2 Particle Size

detected alterations could be the result of the reduced strength of the blue discharge brought on by greater rear-dispersion and repeated absorbance, as well as the variation in color allocation. It should be mentioned that the phosphor sheet usually has a broader width as particle size grows, which reduces the energy of the entire hue range. The illumination transformation among blue and yellow or red-orange will therefore be more noticeable. This suggests that for exceptionally big particle sizes, the transmuted beam might engage in rear-reflection, which would lower the light intensity and result in an increased CCT value.

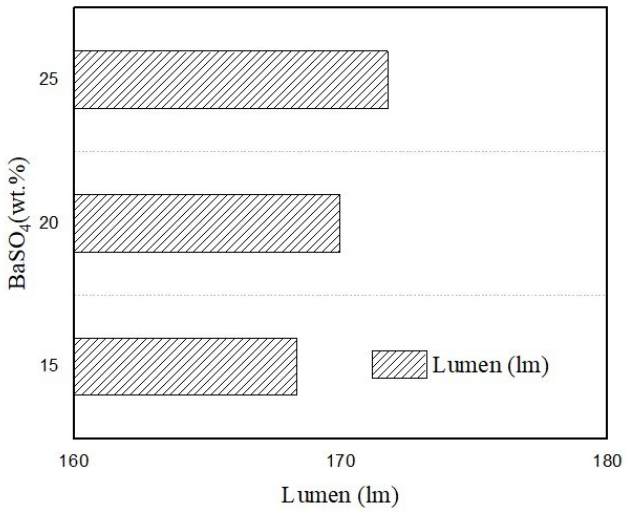

Figure 6. LED Lumen Generated Based on SiO_2 Particle Size

The color generating output of the WLED device is also affected by the particle size. As the particle size increases, CRI and CQS show slight decreases in Figures 7 and 8. Numerous crashes that have been seen could be caused by the color variation among the orange-yellow, blue, and green components. This disparity arises because the discharge color of the rays frequently favors the orange-yellow zone, and greater dispersion with bigger particle sizes results in more orange-yellow parts. As a consequence, decreased CRI and CQS may arise from excessive dispersion.

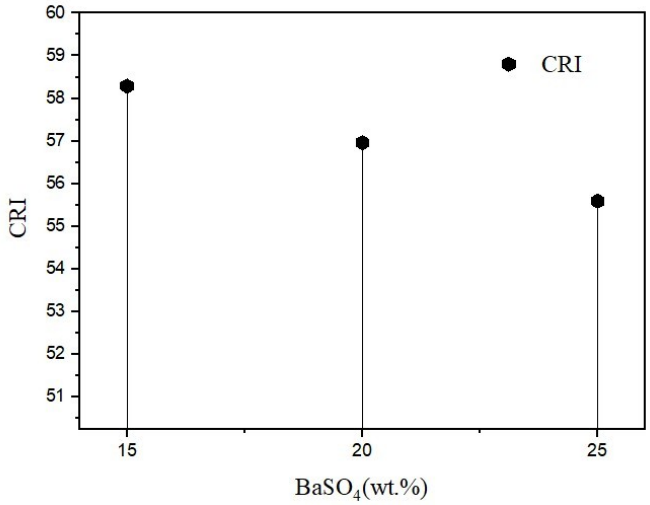

Figure 7. CRI Values with Various SiO_2 Proportions

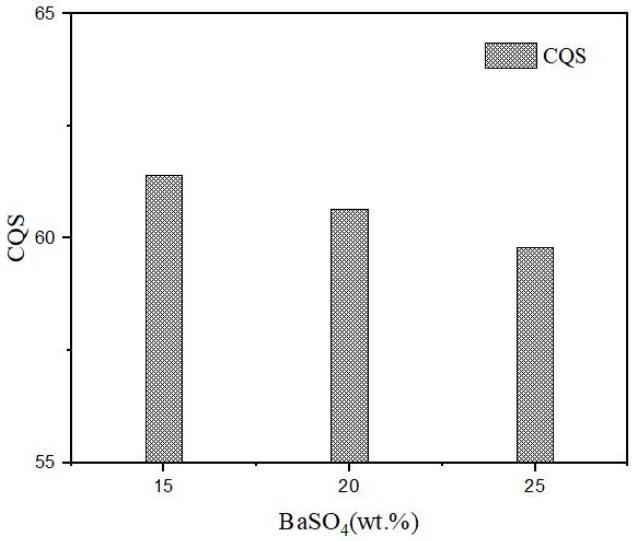

Figure 8. CQS Values with Various SiO_2 Proportions

When it comes to hue quality measurement, CRI is the most widely used and traditional indicator. CRI evaluates eight hue samples under testing illumination and natural illumination, then contrasts the conditions to determine hue quality. When evaluating hue effectiveness under wide-spectrum illumination, CRI is helpful. Nevertheless, this index was created long before LED devices were produced, thus it cannot be used with them. The resulting desaturation would be too great to properly evalu-

ate the chromaticity from LED devices utilizing just the few hue specimens from CRI. By evaluating fifteen hue specimens, CQS was designed to address this flaw and produce more accurate hue evaluations. CQS takes into account individual taste and hue discrepancy in addition to additional hue specimens. CQS would be a more appropriate index for analyzing the color efficiency of contemporary devices like LEDs since it was developed more recently.

4. CONCLUSIONS

The ZOEF nanogranules were created via the solid-state approach. Through testing, ZrO_2 granules ended up being partly fixated within the strong symmetric polymorphic stage. The PL spectra for every assessed granule subject to excitation comprise extensive bar for host-associated blue-green discharge as well as noticeable apexes for red discharge matching radioactivity shifts within the Eu granules. The PL exciting spectra for Eu^{3+} discharge comprise charge shift bar between O^{2-} and Eu^{3+} under apexes linked with electronic shifts between ground status and excited statuses for Eu^{3+} granules. Fluorization for Eu-integrated ZrO_2 lessens the host-associated PL intenseness as well as boosting the Eu^{3+} luminescent intenseness at least sixfold regarding the sample not featuring fluorine. The greatest Eu PL intenseness was seen in the case of ZOEF nanogranules. The perceived influence would be clarified alteration in oxygen as well as ZrO_2 opening quantity under surging fluorine presence within ZOEF granules. The ZOEF granules would be proper luminescent substances applicable to LEDs. It is possible to modify the substances' intenseness as well as hue coordinate via variance in Eu as well as fluorine presence. The subsequent research for ZOEF nanogranules would be paramount for validating proposed speculations.

5. ACKNOWLEDGEMENT

The authors wish to express their gratitude to the Posts and Telecommunications Institute of Technology, Vietnam, for financial support for this research.

REFERENCES

Anh, N. D. Q. (2024). Nano Scattering Particle: An Approach to Improve Quality of the Commercial LED. *The University of Danang - Journal of Science and Technology*; 53–57

Anh, N. D. Q., S. D. Ho, P. T. M. Man, T. K. Duy, and N. T. P. Loan (2025). Obtaining Higher LED's Lighting Chromaticity and Luminosity with SiO_2 Particles at Different Diameters. *Journal of Advanced Engineering and Computation*, **9**(1); 21

Cong, P. H. and N. D. Q. Anh (2025). Augmenting Chroma Performance for WLED Employing $Sr_8ZrSc(PO_4)_7:Eu^{2+}@SiO_2$ as a Scattering-Enhancing Substance. *Science & Technology Indonesia*, **10**(2); 467–472

Cong, P. H., N. T. P. Loan, N. D. Q. Anh, and H. Lee (2025). Influence of Potassium Bromide Phosphor on Optical Properties of White Light-Emitting Diodes. *International Journal of Advances in Applied Sciences*, **14**(4); 1359

Dang, H. P., P. T. That, and N. D. Q. Anh (2021). Utilizing $CaCO_3$, CaF_2, SiO_2, and TiO_2 Phosphors as Approaches to the Improved Color Uniformity and Lumen Efficacy of WLEDs. *TELKOMNIKA (Telecommunication Computing Electronics and Control)*, **19**(2); 623

Dung, N. V. and N. D. Q. Anh (2025). $Ba_3GdNa(PO_4)_3F:Eu^{2+}$ Phosphor with Blue-Red Emission Colors on White-LED Properties. *Indonesian Journal of Electrical Engineering and Computer Science*, **38**(3); 1564

Hanh, N., P. That, N. D. Q. Anh, and T. Trang (2021). Triple-Layer Remote Phosphor Structure: A Novel Option for the Enhancement of WLEDs' Color Quality and Luminous Flux. *Materials Science-Poland*, **38**(4); 654–660

Le, P., S. Ho, N. D. Q. Anh, and H.-Y. Lee (2022). Triple-Layer Remote Phosphor Structure: A Potential Packaging Configuration to Enhance Both Color Quality and Lumen Efficiency of 6,000–8,500 K WLEDs. *Materials Science-Poland*, **39**(4); 458–466

Le, P. X., N. T. P. Loan, and N. D. Q. Anh (2026). Optical Assessment of Titanium Oxide Employed in Phosphor-Transmuted WLED Devices. *Science & Technology Indonesia*, **11**(1); 345–355

Le, P. X., N. T. P. Loan, N. D. Q. Anh, and H. Lee (2025). Thermally Stable Sol-Gel Yttrium Aluminum Garnet Cerium Phosphors for White Light-Emitting Diodes. *International Journal of Advances in Applied Sciences*, **14**(4); 1367

Loan, N. T. P., N. D. Q. Anh, P. T. M. Man, and H. Lee (2025). Assessing Thermic Degradation for Yttrium–Aluminum Precursive Agents Applied to YAG Phosphor Samples. *Science & Technology Indonesia*, **10**(4); 1209–1214

Luo, G. F., N. Loan, L. Tho, P. That, N. D. Q. Anh, M. J. Chen, H. Y. Liao, and H. Y. Lee (2020a). Building Superior Lighting Properties for WLEDs Utilizing Two-Layered Remote Phosphor Configurations. *Materials Science-Poland*, **38**; 493–501

Luo, G. F., N. T. P. Loan, L. V. Tho, N. D. Q. Anh, and H. Y. Lee (2020b). Enhancement of Color Quality and Luminous Flux for Remote-Phosphor LEDs with Red-Emitting $CaMgSi_2O_6:Eu^{2+},Mn^{2+}$. *Materials Science-Poland*, **38**(3); 409–415.

Ma, H. and N. D. Q. Anh (2024). Review the Influence of Aluminum–ZnO Films on Multi-Chip Remote-Phosphor White LEDs' Properties. *Journal of Advanced Engineering and Computation*, **8**(4); 225

That, P. T., T. M. Bui, N. T. P. Loan, P. X. Le, N. D. Q. Anh, and L. V. Tho (2020). Dual-Layer Remote Phosphor Structure: A Novel Technique to Enhance the Color Quality Scale and Luminous Flux of WLEDs. *International Journal of Electrical and Computer Engineering*, **10**(4); 4015–4022

Thi, M. H. N., N. T. P. Loan, and N. D. Q. Anh (2020a). Acquiring Higher Lumen Efficacy and Color Rendering Index with Green $NaYF_4:Er^{3+}Yb^{3+}$ and Red α-$SrO{\cdot}3B_2O_3:Sm^{2+}$ Layers for Designing Remote Phosphor LED. *TELKOMNIKA (Telecommunication Computing Electronics and Control)*, **18**(6); 3222

Thi, M. H. N., N. T. P. Loan, and N. D. Q. Anh (2020b). Study of Red-Emitting $LaAsO_4:Eu^{3+}$ Phosphor for Color Rendering Index Improvement of WLEDs with Dual-Layer Remote Phos-

phor Geometry. *TELKOMNIKA (Telecommunication Computing Electronics and Control)*, **18**(6); 3210

Trang, L. T. and N. D. Q. Anh (2025). Influences from SiO_2 Particles on Optical Properties of White Diodes Verified Through Computer Simulation. *Indonesian Journal of Electrical Engineering and Computer Science*, **38**(3); 1572

Trang, L. T., N. T. P. Loan, P. H. Cong, N. D. Q. Anh, and H. Lee (2025). Computer Simulation and Software Engineering in Optical Analysis of Phosphor-Converted White Light-Emitting Diodes Utilizing Barium Sulfate. *International Journal of Advances in Applied Sciences*, **14**(4); 1384

Trang, T. T. (2022). Comparison Between SEPs of $CaCO_3$ and TiO_2 in Phosphor Layer for Better Color Uniformity and Stable Luminous Flux of WLEDs with 7,000 K. *Materials Science-Poland*, **40**; 1–8

